Structural modification in molten metal chloride and alkali chloride mixtures

1993 J. Phys.: Condens. Matter 5 7189

(http://iopscience.iop.org/0953-8984/5/39/007)

J. Phys.: Condens. Matter 5 (1993) 7189–7202. Printed in the UK

Structural modification in molten metal chloride and alkali chloride mixtures

Y S Badyal and R A Howe

Department of Physics and Astronomy, University of Leicester, Leicester LE1 7RH, UK

Received 11 May 1993

Abstract. Structure factors have been measured by time-of-flight neutron diffraction for $NiCl_2$–KCl, $NiCl_2$–LiCl and $ZnCl_2$–LiCl binary molten salt mixtures. The results are consistent with those from earlier thermodynamic and spectrophotometric studies, in which the degree of structural modification was found to depend on the type of alkali cation. The $NiCl_2$–LiCl and $ZnCl_2$–LiCl systems appear to be almost ideal admixtures of the pure salts. However, adding KCl to $NiCl_2$ results in enhancement of the local structure and intermediate range order. The first sharp diffraction peak at $Q \simeq 1$ Å^{-1} in pure $NiCl_2$, which is more prominent than previously reported, appears to be enhanced by the addition of KCl up to a high concentration of alkali halide. No change is apparent in $NiCl_2$–LiCl or $ZnCl_2$–LiCl.

1. Introduction

Extensive studies have been undertaken of the structural properties of pure molten salts, motivated by an interest in the thermodynamic, electrochemical and transport properties. In practical terms however, molten salt mixtures are of far greater commercial significance. The comparative lack of structural information on such mixtures is due, in part, to the increased complexity of binary salt systems. For a pure molten salt the structure can be described in terms of three partial structure factors and the corresponding radial distribution functions. For a general binary mixture containing four ion species, ten partial structure factors are needed (although this number can be reduced to six if a cation or anion species is common to both salts). We report on a study of the structure of binary mixtures of molten chlorides.

There have been a number of studies, by several techniques, of binary molten salt mixtures with the general formula MX_2–AX (where M is a divalent metal, A is an alkali metal and X the common halide). Thermodynamic measurements indicate deviations from random mixing and the common formation in these systems of mainly tetrahedral MX_4^{2-} complexes at $\frac{2}{3}$ alkali halide concentration, with the degree and stability of complexing dependent on the size of alkali cation. Enthalpies of mixing data [1] for $NiCl_2$–ACl (A = Li, Na, K, Rb and Cs) suggest that these mixtures exhibit strong deviations from ideality for the larger alkalis such as Cs, Rb and K, less so for Na and almost not at all for Li. Entropies of mixing [2] are also consistent with the formation of well-ordered, energetically stable tetrahedral units with the reduction in partial molar entropy most pronounced for the largest alkali metal.

Optical absorption spectra for a transition metal ion like Ni^{2+} are sensitive indicators of the coordination geometry because the energy levels of the poorly shielded 3d electrons are strongly influenced by the local environment. In spectrophotometric measurements of

0953-8984/93/397189+14$07.50

$NiCl_2$–ACl melts [3, 4], the characteristic absorption spectra of $NiCl_4^{2-}$ becomes increasingly evident as the size of the alkali cation is increased from Li to Cs. X-ray diffraction measurements show that the nickel atoms are almost all tetrahedrally coordinated in crystalline $Cs_3(NiCl_4)Cl$ so the similarity of the absorption spectra for solid and liquid phases of the compound provides evidence for the existence of the tetrahedral $NiCl_4^{2-}$ unit in the melt [5]. Optical absorption studies [6] of dilute ternary solutions of $NiCl_2$ in KCl–LiCl reveal that adjusting the proportions of the two alkali halides affects the coordination geometry of the Ni^{2+} ion in a systematic way. Increasing KCl results in predominantly tetrahedral structural units whereas more LiCl leads to a less regular, probably octahedral geometry.

Theoretical models, such as the simple complex anion model of Pelton [7], have been proposed which can reproduce the general features of the experimental enthalpies and entropies of mixing curves. These models attempt to explain the thermodynamic data solely in terms of the degree of complexing and ordering of the local structure of the metal cation. The question arises as to whether any of the reduction in entropy and enthalpy observed in these mixtures is due to structural correlations between complex units namely intermediate range order (IRO). The presence of a first sharp diffraction peak (FSDP) at $Q \simeq 1$ Å^{-1} in the diffraction data for MX_2 melts with small cations has been taken as evidence of IRO arising from linked structural units. In the 'network liquid' model [8] (and references therein) proposed for the $ZnCl_2$ melt, correlations between corner sharing neighbouring units are thought to lead to correlations between the cations at the centres of these units. This model implies that adding alkali halide would break up the IRO and allow isolated structural units to be formed by reducing the need for anion sharing.

In order to obtain direct evidence of the structural modification of MX_2 salts by different alkali halides as indicated in previous studies, time-of-flight (TOF) neutron diffraction experiments were carried out on molten $NiCl_2$–KCl, $NiCl_2$–LiCl and $ZnCl_2$–LiCl samples covering a range of compositions. The availability of partials information for the pure salts and the dissimilarity in their total scattering functions makes it possible to interpret the mixtures' data without using isotopic substitution. For example the size and position of the FSDP can be followed as a function of composition to obtain information about the state of IRO in the mixtures.

2. Theoretical background

The quantity measured in a neutron diffraction experiment is the total structure factor $F(Q)$. This is defined for a two-component system with atoms of type a and b by the following relation:

$$F(Q) = c_a^2 b_a^2 (S_{aa}(Q) - 1) + c_b^2 b_b^2 (S_{bb}(Q) - 1) + 2c_a c_b b_a b_b (S_{ab}(Q) - 1) \quad (1)$$

where c_α is the concentration and b_α is the coherent scattering length of species α. The $S_{\alpha\beta}(Q)$ terms are the partial structure factors according to the definition of Faber and Ziman [9]. The partial structure factor is related to the pair distribution function $g_{\alpha\beta}(r)$ by Fourier transformation as shown below:

$$g_{\alpha\beta}(r) = 1 + \frac{1}{2\pi^2 \rho_0} \int_0^\infty Q^2 (S_{\alpha\beta}(Q) - 1) \frac{\sin(Qr)}{Qr} \, dQ \quad (2)$$

where ρ_0 is the number density. Substitution of (2) into (1) leads to an expression for the Fourier transform (FT) of $F(Q)$ known as the total pair distribution function, or $G(r)$:

$$G(r) = 1 + c_a^2 b_a^2 (g_{aa}(r) - 1) + c_b^2 b_b^2 (g_{bb}(r) - 1) + 2c_a c_b b_a b_b (g_{ab}(r) - 1). \quad (3)$$

Not surprisingly, $G(r)$ is a linear sum of the various partial structures, weighted for concentration and scattering, just as in the original $F(Q)$. The precise form of the equations shown is only valid for pure molten salts such as $NiCl_2$ with two types of atom. However, the molten salt mixtures studied contain three components, so there are six partial structures to be considered.

3. Experimental details

The mixtures were prepared from anhydrous pure ($\geqslant$ 99.99%) single salts heated gently under vacuum to minimize moisture content. Details of the sample preparation procedure are given by Allen *et al* [8]. The lithium chloride used in mixtures with nickel chloride was isotopically enriched ($\geqslant$ 99.99%) in ^{7}Li to avoid the very large absorption cross section for neutrons of the ^{6}Li isotope.

Total structure factors for samples of 0, 20, 40, 55, 70 and 80% KCl with $NiCl_2$ at a temperature of 1040 °C (1050 °C for pure $NiCl_2$) were measured on the LAD instrument at Rutherford ISIS. Samples of 33 and 67% LiCl with $NiCl_2$ were measured at the same temperature. In addition, 0, 33 and 67% LiCl with $ZnCl_2$ compositions were studied at 450 °C. The $F(Q)$ for pure LiCl (at 650 °C) was obtained on ISIS SANDALS. Multiple scans were taken for each sample to check whether structural changes in sample or container, from incomplete mixing or chemical attack, occurred during data collection. Only scans that agreed to within the statistical error were added together. Data were collected for the empty container (at 1040 °C) and furnace backgrounds, and a vanadium calibration was carried out.

The raw data were analysed using the Rutherford ATLAS package [10] in the manner described by Allen *et al* [8]. Some problems were encountered with the data for the $NiCl_2$ mixtures where a marked fall off in scattering with increasing Q gives rise to a large slope in $F(Q)$. This systematic error is proportionately worse at lower detector angles and so appears to be related to neutron energy. It was corrected by fitting a theoretical $G(0)$ base level to the $G(r)$ data and back-transforming to obtain a correction for the original $F(Q)$. However, the large slope has the effect of making renormalization less accurate, leading to a larger than usual error (say 5–10%) in the absolute normalization of the data for the $NiCl_2$ mixtures. The lack of isothermal compressibility data precludes the use of the long wavelength limit $F(0)$ as a check on normalization. The missing low-Q portion of the data was simply extrapolated. This makes little difference to the real-space picture because of the Q^2 dependence of the FT.

The $G(r)$ functions were obtained by Fourier transformation of $F(Q)$ data which were smoothed at high Q. No window function was employed. Comparison of the resulting $G(r)$ with and without smoothing the $F(Q)$ confirmed that it was mainly Fourier ripple that was removed, with marginal effect on real peaks.

The data analysis parameters for the pure salts are given in table 1. Due to the lack of published measurements, number densities for the $NiCl_2$ mixtures were linearly interpolated from those of the pure salt endpoints at 1040 °C. Density data for the $ZnCl_2$–LiCl mixtures (and the pure salts) were obtained from Yoko *et al* [13].

Table 1. Data analysis parameters used for the pure salts. The temperatures corresponding to the density figures are in brackets.

	Number density		FZ coefficients		
Pure salt	ρ_0 (Å^{-3})		M–M	M–Cl	Cl–Cl
$NiCl_2$	0.0367[a]	(1050 °C)	0.118	0.0439	0.408
KCl	0.0223	(1040 °C)	0.034	0.178	0.230
	0.0242	(820 °C)	"	"	"
^7LiCl	0.0375	(1040 °C)	0.012	−0.104	"
LiCl	0.0421	(640 °C)	0.009	−0.091	"
$ZnCl_2$	0.0327	(450 °C)	0.036	0.242	0.408
	σ_c(barns)	σ_s(barns)	σ_a(barns) at 1.8 Å		
Nickel	13.3	18.5	4.49		
Potassium	1.73	1.98	2.1		
Chlorine	11.53	16.7	33.5		
^{7}Lithium	0.62	1.40	0.045		
Lithium	0.45	1.36	70.5		
Zinc	4.05	4.13	1.11		

The scattering cross sections are from Sears [11].
[a] Galka *et al* [12].

4. Discussion

Before considering the mixtures it is instructive to first examine the data for pure $NiCl_2$. Total structure factors from the previous reactor diffraction investigation of Newport *et al* [14] and the current TOF study (henceforth referred to as I and II respectively) are shown in figure 1: clear differences are apparent, even when uncertainty in normalization of the data is taken into account.† In particular, the FSDP in II is larger and more comparable in size to that of molten $NiBr_2$ [15]. If, as several studies indicate [15–17], the FSDP is a signature of directional bonding then a comparison of electronegativity differences suggests the feature should be a similar size in both nickel halides. However, Newport *et al* found only a small contribution to the FSDP from $S_{Ni-Ni}(Q)$: our total scattering data suggest it is as significant as in $NiBr_2$. Since a large FSDP is a consistent feature of the data for the mixtures (as will be seen later) the current data for pure $NiCl_2$ are preferred to that of Newport *et al* in the discussion that follows.

Despite the differences between I and II some real-space parameters remain in agreement and are unambiguous (see table 2). The estimated coordination number is not significantly different and the r_{--}/r_{+-} ratio in $g(r)$ remains almost identical at approximately 1.50. Newport *et al* used the naturally higher value of this ratio in $r^2g(r)$ of $\simeq 1.60$ to support their conclusion that the local structure of molten $NiCl_2$ is approximately tetrahedral. However, reverse Monte Carlo (RMC) simulation [18] suggests that although the local structure is highly disordered in the melt it is probably best characterized as octahedral, as in the crystalline solid, with one–two vacancies. RMC simulation gives a tetrahedral geometry for pure molten $ZnCl_2$ which is again consistent with the known structure of the crystalline solid. Structural parameters for $ZnCl_2$ are shown in table 2 for comparison. The r_{--}/r_{+-} ratios have been calculated *consistently* using peak positions in $g(r)$ and are clearly different for

† NB The Q_{max} indicated in this and other figures (2, 4 and 9) was selected for display purposes, and the actual Q_{max} used in Fourier transformation was typically between 20 and 25 Å^{-1}. In the same figures the extrapolated region below Q_{min} (typically between 0.3 and 0.4 Å^{-1}) is indicated by the smoothness of the curves fitted.

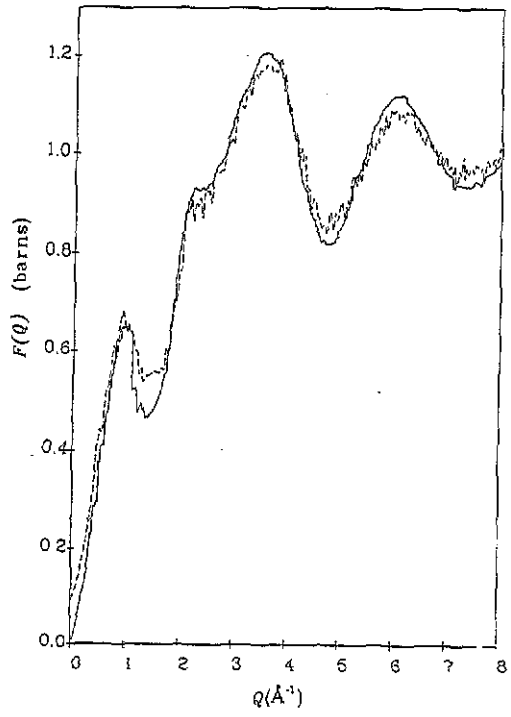

Figure 1. Comparison of total structure factors for molten $NiCl_2$: current study (full curve) and previous study by Newport *et al* [14] (broken curve).

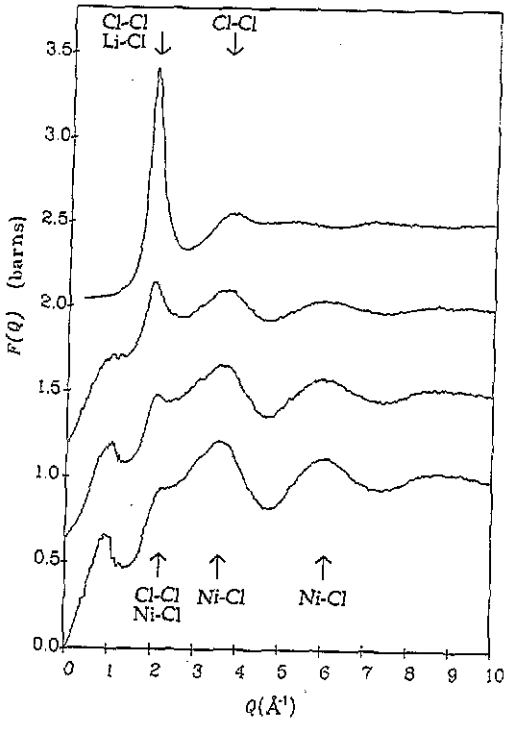

Figure 2. Total structure factors for molten $NiCl_2$–LiCl mixtures. The main partial contributions to prominent peaks in the pure salts are indicated. The LiCl data is from McGreevy [20].

Table 2. Comparison of real-space structural parameters for pure $NiCl_2$ and $ZnCl_2$ [19]. The coordination number is for the anions around each metal cation.

	$NiCl_2$ I	$NiCl_2$ II	$ZnCl_2$
Coordination number	4.7 ± 0.2	4.4 ± 0.2	4.3 ± 0.3
r_{M-Cl}	2.32 ± 0.02	2.28 ± 0.02	2.29 ± 0.02
r_{Cl-Cl}	3.48 ± 0.02	3.40 ± 0.02	3.71 ± 0.02
r_{--}/r_{+-}	1.50 ± 0.03	1.49 ± 0.03	1.62 ± 0.03

the two salts. It seems unlikely that they share a similar geometry, as suggested by Newport *et al* .

The value of the r_{--}/r_{+-} ratio for pure $ZnCl_2$ is in good agreement with the theoretical $\sqrt{8}/3$ ($\simeq 1.63$) expected for a regular close-packed tetrahedron and is consistent with the RMC result. The ratio for pure $NiCl_2$ is about halfway between that for a regular tetrahedron and an octahedron ($\sqrt{2} \simeq 1.41$). This is also consistent with the RMC result. A disordered octahedral structure with on average almost two vacancies (hence a mean coordination number close to four) and distorted bond angles begins to resemble a distorted tetrahedral structure, which explains the intermediate value of the ratio. Since the RMC method fits a physical model to the whole of the data, it is inherently more reliable as a guide to local structure than any method based on particular features of the $G(r)$ data, such as peak positions. However, it does seem that the r_{--}/r_{+-} ratio in $g(r)$, taken together with the coordination number, indicates local geometries consistent with those from the RMC†.

In the discussion of the mixtures data which follows, the local structure of pure $NiCl_2$ is taken to be irregular, but probably best described as distorted octahedral with one–two vacancies on average. Although some structural parameters agree, because of the inconsistencies between I and II, interpretation of the data for the $NiCl_2$ mixtures is based primarily on a consideration of the trends in peak position, height etc. as a function of composition rather than the absolute values. The RMC technique was not used because the constraint of a single $F(Q)$ dataset for each composition was not expected to yield structures sufficiently unambiguous to be useful in extending the analysis of such complex molten salt systems.

4.1. The structure of molten $NiCl_2$–LiCl and $ZnCl_2$–LiCl

Total structure factors and real-space functions for the $NiCl_2$–LiCl mixtures are given in figures 2 and 3 respectively. The corresponding data for the $ZnCl_2$–LiCl mixtures are presented in figures 4 and 5. Both systems appear to exhibit simple admixture behaviour. A gradual change with composition in size and position of characteristic features of the pure salts is readily apparent in $F(Q)$.

The metal and alkali cations appear to retain their pure salt local structures in the mixtures. In real space the positions of the principal peaks from $g_{Ni-Cl}(r)$ or $g_{Zn-Cl}(r)$ overlap almost exactly with $g_{Li-Cl}(r)$ (the Ni^{2+}, Zn^{2+} and Li^{+} ions are very similar in size) so the contributions of the two partials cannot be easily distinguished. However, the normalized height H_c of the combined first peak in $G(r)$, which is defined by the equation

$$H_c = c_M b_M (g_{M-Cl}(r) - 1) + c_{Li} b_{Li} (g_{Li-Cl}(r) - 1) \tag{4}$$

† Using the positions of peaks in $r^2 g(r)$ to calculate r_{--}/r_{+-} would at first sight seem more correct. However, all such methods neglect the effect of vacancies in the structure which would particularly affect the r_{--} position in $r^2 g(r)$ leading to an over-estimate of the true ratio relating to the local structure. The RMC solution includes the effect of vacancies through the use of the density constraint and consequently gives a more meaningful result. It should be noted that the ratio in $r^2 g(r)$ for $ZnCl_2$ is about 1.7 which does not correspond to any obvious geometry.

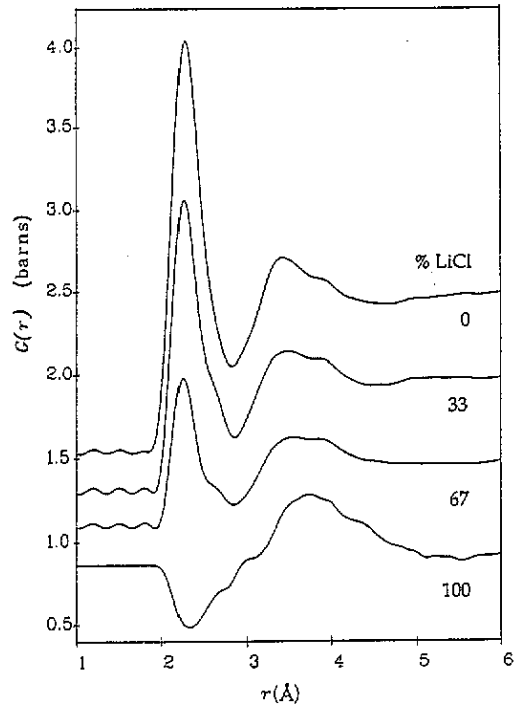

Figure 3. Total pair distribution functions for molten $NiCl_2$–LiCl mixtures.

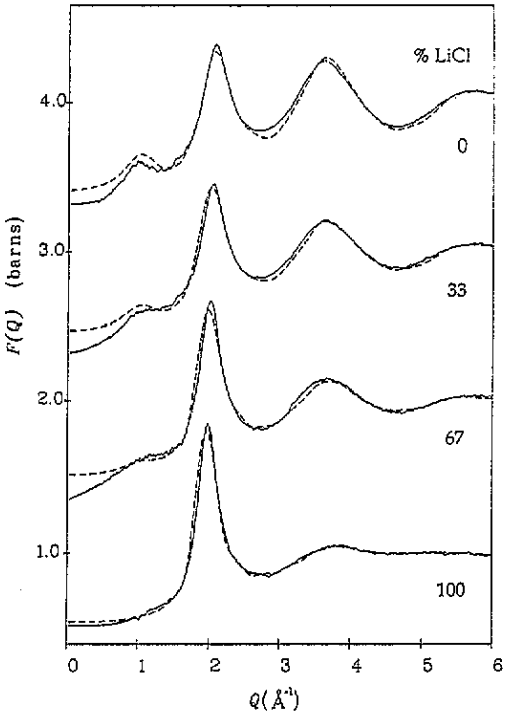

Figure 4. Comparison of $F(Q)$ data for $ZnCl_2$–LiCl (full curve) against model total structure factors (broken curve) generated from the pure salt partials. The $ZnCl_2$ partials are from Biggin and Enderby [19] and for LiCl from McGreevy and Howe [20]. The divergence at low Q is probably due to the lack of a furnace correction in our data.

where M is the metal species, can be estimated and is shown as a function of composition in figure 6. A linear plot is to be expected if both partials remain unchanged in size and position between the endpoints. The results are clearly linear for $ZnCl_2$–LiCl and seem to be linear also for $NiCl_2$–LiCl. In the case of the latter, uncertainty in number density and inconsistencies in the absolute normalization of the data explains most of the deviation.

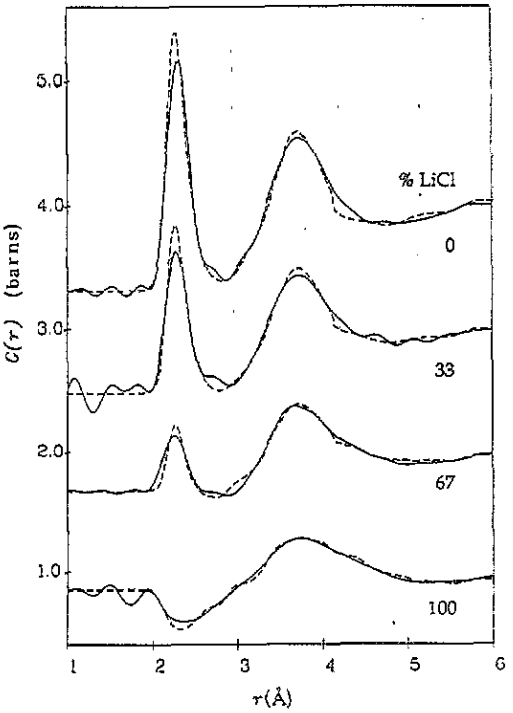

Figure 5. Comparison of $G(r)$ data for $ZnCl_2$–LiCl (full curve) against model total pair distribution functions (broken curve) from the pure salt partials. The discrepancy between model and data at the principal peak can be explained by the difference in temperature and the effects of Fourier ripple.

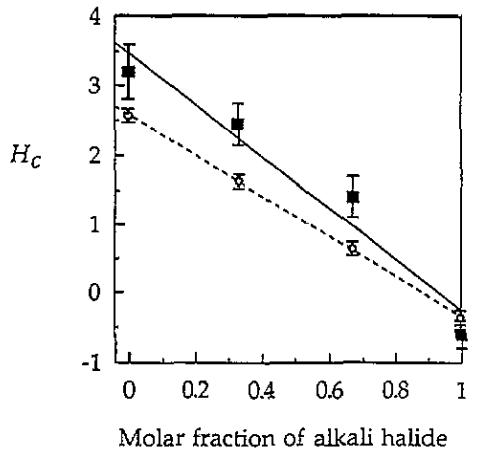

Figure 6. Normalized height H_c (equation (4)) of the principal peak in $G(r)$ as a function of alkali halide concentration: $NiCl_2$–LiCl (■ and full curve) and $ZnCl_2$–LiCl (○ and broken curve). Least-squares linear best fits are shown for the two systems.

Each type of cation has a characteristic anion structure so the second peak in $G(r)$ may be modelled as the weighted average of two pure salt partials—$g^{LiCl}_{Cl-Cl}(r)$ and $g^{MCl_2}_{Cl-Cl}(r)$ (the superscript refers to the pure salt). For the $NiCl_2$–LiCl mixtures the position r_{Cl-Cl} of the

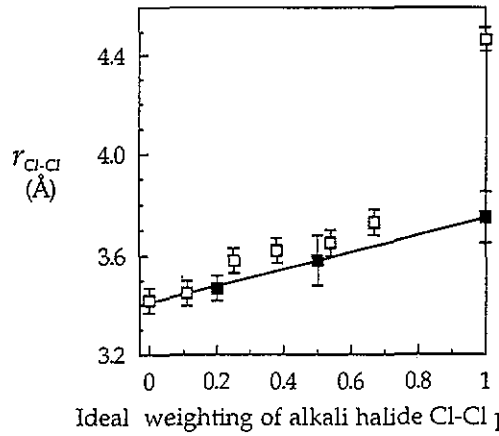

Figure 7. Position of the anion–anion peak r_{Cl-Cl} as a function of *ideal* weighting of the alkali halide $g_{Cl-Cl}(r)$ partial: $NiCl_2$–KCl (□) and $NiCl_2$–LiCl (■).

anion–anion peak in $G(r)$ has been plotted against the *ideal* weighting, i.e. according to the ratio of chlorine in the pure salts, of the $g^{LiCl}_{Cl-Cl}(r)$ partial in figure 7. The excellent linear fit indicates simple averaging of the pure salt anion structures and is of course consistent with little or no change in local structure for both types of cation. Modelling the data for the $ZnCl_2$–LiCl mixtures using the pure salt partials† [19, 20] weighted with the appropriate Faber–Ziman (FZ) coefficients supports a similar conclusion for this system. Good fits to the anion–anion peak at $r \simeq 3.75$ Å are achieved using the *ideal* weighting of $g^{LiCl}_{Cl-Cl}(r)$ and $g^{ZnCl_2}_{Cl-Cl}(r)$. Although the primary peak in both partials is at virtually the same position there is a significant difference in height so the fit does give an indication of the correctness of weighting.

The results also suggest that admixture behaviour extends to the FSDP and hence IRO. The estimated height H_p of the $S_{Ni-Ni}(Q)$ contribution to the FSDP is plotted against composition for the $NiCl_2$–LiCl mixtures in figure 8. H_p is defined as:

$$H_p = (H_Q - c_{Ni}c_{Cl}b_{Ni}b_{Cl}(0.4))/(c_{Ni}b_{Ni})^2 \tag{5}$$

where H_Q is the total height of the FSDP in $F(Q)$. The contribution from $S_{Ni-Cl}(Q)$, which is assumed to remain unchanged from its value of about 0.4 ± 0.2 in pure $NiCl_2$, is subtracted from H_Q to give the FSDP from $S_{Ni-Ni}(Q)$ alone. The results, despite the large error bars, suggest H_p remains approximately constant. As regards the $ZnCl_2$–LiCl system, H_Q may be estimated in a consistent manner for both model and data and compared directly. The almost exact agreement obtained suggests that the contributions to the FSDP from both $S_{Zn-Zn}(Q)$ and $S_{Zn-Cl}(Q)$ simply scale with the FZ coefficients across the composition range.

Despite the differences in local structure between $ZnCl_2$ and $NiCl_2$ both salts exhibit a similar admixture behaviour with LiCl. The almost identical size of the Ni^{2+} and Zn^{2+} ions (with the alkali cation being only slightly smaller) prompts an explanation based on size and polarizing power. In the pure 2:1 salts each metal cation is competing for influence over surrounding anions with identical next-nearest-neighbour cations. As more LiCl is added these neighbours are increasingly likely to be alkali rather than metal cations, but

† The unknown Zn–Li partial has a small Faber–Ziman coefficient so it could be safely omitted.

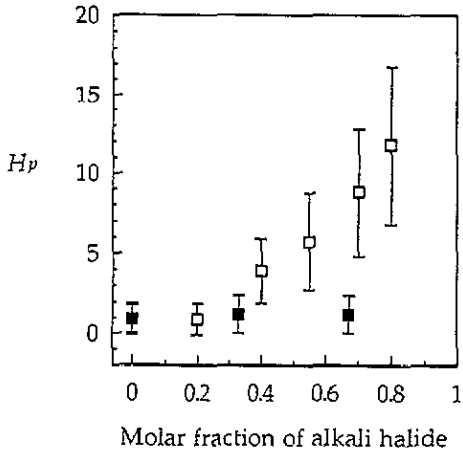

Figure 8. Estimated height H_p of the $S_{Ni-Ni}(Q)$ contribution to the FSDP as a function of alkali halide concentration: $NiCl_2$–KCl (□) and $NiCl_2$–LiCl (■).

there is apparently little effect on local structure even though doubly charged ions have been replaced by singly charged ones. However, the fractional number density of cations in pure LiCl is about twice that in the metal chlorides. This implies that in the mixtures the local concentration of Li^+ neighbours of Ni^{2+} or Zn^{2+} ions is also about twice what might be expected from simple replacement of metal cations. Thus the lower polarizing power of singly charged alkali cations is compensated for by the greater numbers of such ions. The lack of structural modification in the mixtures with LiCl is consistent with thermodynamic data for enthalpies and entropies of mixing for these and other MCl_2–LiCl systems where there is little or no deviation from ideality.

4.2. Structural modification in $NiCl_2$–KCl

Total structure factors and corresponding real space functions for the $NiCl_2$–KCl mixtures are shown in figures 9 and 10. In contrast to the LiCl mixtures, addition of KCl to $NiCl_2$ results in clear deviation from simple admixing of the two pure salt structures. Characteristic features of pure $NiCl_2$ remain prominent in $F(Q)$, even up to 80% KCl.

The results indicate not just persistence but actual enhancement of the $NiCl_2$ local structure in the mixtures. In real space the principal peak from $g_{Ni-Cl}(r)$ remains prominent at the same position up to the highest KCl concentration. The $g_{Ni-Cl}(r)$ partial has been estimated for each composition by assuming that all the other partials in the expression for $G(r)$ (equation (3)) are approximately zero at short distances. Structural parameters for partials generated by this method are given in table 3. The height of the principal peak in 80% KCl is about 30% greater than in pure $NiCl_2$ and there is some reduction in the FWHM. In addition, a gradual shift in the position of the first minimum to lower r with increasing KCl concentration is apparent. However, the position of the first minimum will be affected by the gradual emergence of the principal peak from $g_{K-Cl}(r)$ which will also tend to shift the minimum down to lower r. When full account is taken of the effect of $g_{K-Cl}(r)$ some shift to lower r is still evident and in addition there is a continuous reduction in height of the feature. It is apparent from this that in the presence of K^+ ions the local structure of the Ni^{2+} ion becomes better defined with less ionic exchange into and out of the first coordination shell.

The results also indicate a gradual change in the local geometry of the metal cation in the mixtures. There is a continuous shift in the position r_{Cl-Cl} of the anion–anion peak in $G(r)$ from its characteristic value in pure $NiCl_2$ to higher r with increasing KCl (figure 7). This is

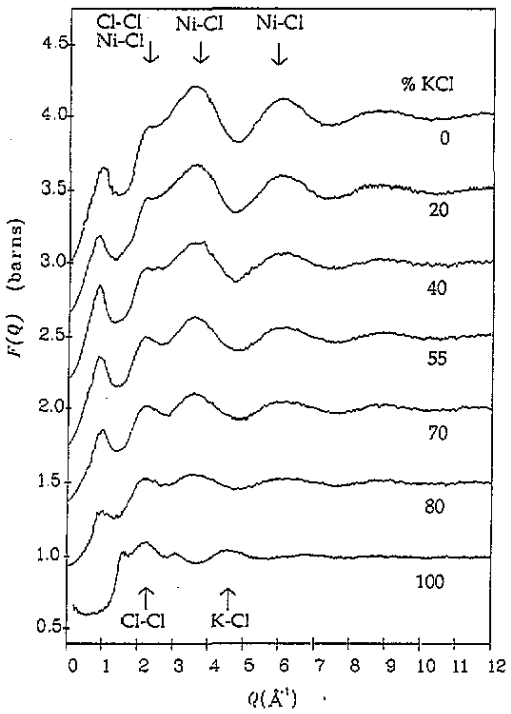

Figure 9. Total structure factors for the molten $NiCl_2$–KCl mixtures. The main partial contributions to prominent peaks in the pure salts are indicated.

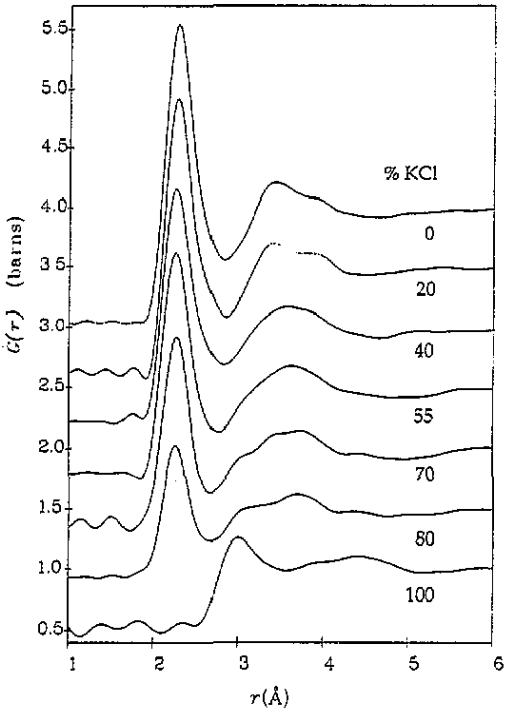

Figure 10. Total radial distribution functions for molten $NiCl_2$–KCl mixtures.

Table 3. Structural parameters for the estimated $g_{Ni-Cl}(r)$ partials. All parameters refer to $4\pi\rho_0 r^2 g(r)$. The coordination number is for the anions around nickel.

	Principal peak		First min.	Coordination number by integration over $r^2g(r)$		
	position	height	position			
% KCl	(Å)	(Å^{-1})	r_{min}(Å)	(symmetric)	(to r_{min})	FWHM
0	2.28 ± 0.02	14 ± 1.25	2.80 ± 0.02	3.4 ± 0.4	4.4 ± 0.1	0.42 ± 0.04
20	2.27 ± 0.02	14 ± 1.25	2.82 ± 0.02	3.1 ± 0.4	4.3 ± 0.1	0.42 ± 0.04
40	2.26 ± 0.02	14 ± 1.5	2.79 ± 0.02	3.1 ± 0.4	4.2 ± 0.1	0.45 ± 0.04
55	2.25 ± 0.02	16 ± 1.7	2.75 ± 0.05	3.5 ± 0.4	4.25 ± 0.05	0.42 ± 0.04
70	2.27 ± 0.02	18 ± 2.2	2.65 ± 0.05	3.9 ± 0.5	4.1 ± 0.1	0.37 ± 0.04
80	2.26 ± 0.02	18 ± 2.7	2.64 ± 0.05	3.5 ± 0.4	4.1 ± 0.15	0.37 ± 0.04

clearly a trend in the average Cl–Cl separation associated with the local structure of the Ni^{2+} ion since the characteristic peak for pure KCl occurs at much higher r. The large difference in peak positions for the pure salts eliminates any possibility of the effect being due to averaging of the pure salt anion strucures. Since the position of the principal peak remains unchanged the trend in r_{Cl-Cl} implies a gradual change in local geometry. The r_{--}/r_{+-} ratio in $G(r)$ (table 4) gradually increases to reach a value close to that found for pure $ZnCl_2$ at the higher KCl concentrations. The local geometry of the Ni^{2+} ion thus appears to change from a distorted octahedron (with vacancies) to almost regularly tetrahedral. The decrease in coordination number (integrating to r_{min}; see table 3) from approximately 4.4 in pure $NiCl_2$ to 4.1 at 80% KCl seems to be consistent with such modification of the local geometry.

Table 4. The r_{--}/r_{+-} ratios in $G(r)$ for the $NiCl_2$–KCl mixtures.

% KCl	0	20	40	55	70	80
r_{--}/r_{+-}	1.50 ± 0.03	1.52 ± 0.03	1.58 ± 0.03	1.61 ± 0.03	1.61 ± 0.03	1.65 ± 0.03

The height of the anion–anion peak in $G(r)$, associated with the Ni^{2+} ion, stays approximately constant up to high alkali halide concentration when scaled by the *unweighted* FZ coefficient for $g_{Cl-Cl}(r)$. In contrast, the anion–anion peak of pure KCl is diminished even at 80% alkali halide. These observations are evidence that a more stable and ordered local structure for the Ni^{2+} ion is attained at the expense of the K^+ ion and highlight the dominance of the nickel cation in the mixtures. The observations are also consistent with the formation of *isolated* structural units centred on Ni^{2+} ions with the surrounding K^+ ions occupying disordered sites. Isolated structural units imply reduced overlap of the second shell with the first in $g_{Ni-Cl}(r)$ which is consistent with a reduction in height of the first minimum.

Taken together the above findings suggest that adding KCl to $NiCl_2$ promotes the formation of stable, well-ordered, isolated and mainly tetrahedral $NiCl_4^{2-}$ structural units. An explanation for this can be given, as with the LiCl mixtures previously, in terms of the relative size and polarizing power of the two cation species present. The large K^+ ion is almost twice the size of the Ni^{2+} ion and is comparatively weakly polarizing. Consequently the nearest-neighbour K^+ ions around each Ni^{2+} ion cannot compete as effectively for influence over the surrounding anions. The result is a stronger and more stable local structure for the metal cation and conversely a weaker structure for the alkali ion. The large

K^+ ions would also be less effective at shielding the anions from their mutual electrostatic repulsion. This would lead to a tendency for the mean Cl–Cl separation to increase and thus favour a tetrahedral geometry for the local structure of the Ni^{2+} ion. The physical size of the alkali cation would also cause a spacing apart and isolation of the $NiCl_4^{2-}$ units and may be partly responsible for the observed increase in r_{Cl-Cl}. The findings for $NiCl_2$–KCl are in good agreement with those from previous thermodynamic and optical absorption studies.

4.3. The effect of the alkali cation on intermediate range order

There is a contrasting effect on IRO in the mixtures depending on the type of alkali cation. The estimated height H_p of the contribution from $S_{M-M}(Q)$ to the FSDP appears to remain almost constant in $NiCl_2$–LiCl and $ZnCl_2$–LiCl whereas in $NiCl_2$–KCl it increases right up to the highest alkali halide concentration (figure 8). Such apparent enhancement is surprising since the addition of KCl also seems to promote the formation of isolated structural units and a reduction in Ni–Cl–Ni bridging. This implies that either IRO in pure $NiCl_2$ (and perhaps other MX_2 salts) does not arise from the need for anion sharing and the resulting structural correlations between units or that there is a different mechanism for IRO in the mixtures. It is of course possible that the increase in H_p is not just due to $S_{Ni-Ni}(Q)$, as assumed, but may have contributions from other partials such as $S_{Ni-K}(Q)$ and possibly $S_{K-K}(Q)$.

The origin of the FSDP has been attributed to the existence of long chains and clusters of electropositive species in several systems. From RMC simulation of molten $ZnCl_2$ McGreevy and Puztai [18] suggested a model involving chains of Zn^{2+} ions giving rise to fluctuations in cation density on a length scale of 5–10 Å and hence a FSDP at $Q \simeq 1$ Å^{-1}. In a neutron diffraction study of the $ZnCl_2$–KCl system, in which enhancement of the FSDP also seems to occur, Allen *et al* [8] suggested this was due to the formation of similar K^+ ion chains between the original Zn^{2+} ion ones in pure $ZnCl_2$. A difficulty with this model is that it seems to depend on some retention of the 'network liquid' structure of pure $ZnCl_2$ even up to high KCl concentration. However, Raman studies [21] clearly indicate the formation of isolated $ZnCl_4^{2-}$ units in the mixtures. Furthermore, the model seems even less credible in the case of $NiCl_2$–KCl since pure $NiCl_2$ cannot be described as a 'network liquid' to begin with.

Another explanation for the FSDP in terms of the random packing of discrete polyatomic units has been suggested by Price *et al* [22]. However, in $NiCl_2$–KCl the isolated structural units appear to be complex anions and truly random packing of these charged entities will not occur. The $NiCl_4^{2-}$ units will inevitably be surrounded by a shell of large K^+ ions acting to space them apart from other similar units. It is proposed that such charge ordering gives rise to a disordered but somewhat lattice-like arrangement. Hence there would be correlations in density between the well-ordered Ni^{2+} ions leading to an enhanced $S_{Ni-Ni}(Q)$ contribution to the FSDP. The model also implies the existence of (probably weaker) correlations involving $S_{Ni-K}(Q)$ and possibly $S_{K-K}(Q)$ so contributions to the FSDP could be expected from these partials too.

5. Summary

The effect of alkali cation type on structural modification in MCl_2–ACl molten salt mixtures has been confirmed by direct structural measurement. With Li as the alkali the results are best described as simple admixtures of the two pure salt structures. In contrast, considerable structural modification is observed with the larger alkali K. The presence of K^+ ions seems

to promote the formation of stable, well-ordered, isolated and mainly tetrahedral $NiCl_4^{2-}$ units. These findings can be understood in terms of the competition between two types of cation species for anions and hence influence over their local structures. The small, highly polarizing Li^+ ions seem to compete equally well with Ni^{2+} or Zn^{2+} metal cations for Cl^- ions so the local structure around each type of cation remains much the same as in the pure salts. However, the large, weakly polarizing K^+ ion is unable to compete effectively with the Ni^{2+} ion. Consequently, the local structure of the Ni^{2+} ion is strengthened at the expense of that of the K^+ ion. Since enhancement of the FSDP is observed in $NiCl_2$–KCl but not in either of the mixtures with LiCl it appears that the K^+ ion also affects IRO. A model has been proposed in which the large K^+ ions act to space apart the $NiCl_4^{2-}$ units giving rise to a less random, more lattice-like structure and hence increased IRO involving the cations.

In order to ascertain the precise contributions of the various partials to the enhanced FSDP in the total scattering, detailed isotopic studies of the $NiCl_2$+2KCl and $ZnCl_2$+2KCl compositions have been undertaken. The results (including the outcome of RMC simulations) will be published in a future paper.

Acknowledgments

We would like to thank the staff at the RAL ISIS facility, particularly Dr W S Howells and Dr A K Soper, for their assistance in data collection and analysis. Thanks also to Dr H Tromp and the isotope preparation unit at the H H Wills laboratory in Bristol and to Dr D A Allen. We gratefully acknowledge the continued support given to this work by the Science and Engineering Research Council and in particular Y S Badyal would like to thank the SERC for awarding him a studentship.

References

[1] Papatheodorou G N and Kleppa O J 1970 *J. Inorg. Nucl. Chem.* **32** 889
[2] Hamby D C and Scott A B 1968 *J. Electrochem. Soc.* **115** 705
[3] Smith G P and Boston C R 1965 *J. Chem. Phys.* **43** 4051
[4] Smith G P and Boston C R 1967 *J. Chem. Phys.* **46** 412
[5] Boston C R, Brynestad J and Smith G P 1967 *J. Chem. Phys.* **47** 3193
[6] Brynestad J, Boston C R and Smith G P 1967 *J. Chem. Phys.* **47** 3179
[7] Pelton A D 1971 *Can. J. Chem.* **49** 3919
[8] Allen D A, Howe R A, Wood N D and Howells W S 1992 *J. Phys.: Condens. Matter* **4** 1407
[9] Faber T E and Ziman J M 1965 *Phil. Mag.* **11** 153
[10] Soper A K, Howells W S and Hannon A C 1989 *Rutherford Appleton Laboratory Report* RAL-89-046
[11] Sears V F 1984 *Atomic Energy of Canada Ltd* Report AECL-8490
[12] Galka J, Moscinski J and Suski L 1972 *J. Chem. Thermodynamics* **4** 849–56
[13] Yoko T, Crescent R, Tsukagoshi Y and Ejima T 1978 *J. Japan Inst. Met.* **42** 1179
[14] Newport R J, Howe R A and Wood N D 1985 *J. Phys. C: Solid State Phys.* **18** 5249
[15] Wood N D and Howe R A 1988 *J. Phys. C: Solid State Phys.* **21** 3177
[16] Allen D A, Howe R A, Wood N D and Howells W S 1991 *J. Chem. Phys.* **94** 5071
[17] Salmon P S 1992 *Proc. R. Soc.* A **437** 591
[18] McGreevy R L and Puztai L 1990 *Proc. R. Soc.* A **430** 241
[19] Biggin S and Enderby J E 1981 *J. Phys. C: Solid State Phys.* **14** 3129
[20] McGreevy R L and Howe M A 1989 *J. Phys.: Condens. Matter* **1** 9957
[21] Ellis R B 1966 *J. Electrochem. Soc.* **113** 485
[22] Price D L, Moss S C, Reijers R, Saboungi M-L and Susman S 1988 *J. Phys. C: Solid State Phys.* **21** 1069